Millimeter-Wave Remote Self-Heterodyne System for Extremely Stable and Low-Cost Broad-Band Signal Transmission

Yozo Shoji, *Member, IEEE*, Kiyoshi Hamaguchi, *Member, IEEE*, and Hiroyo Ogawa, *Member, IEEE*

***Abstract*—We have developed a millimeter-wave remote self-heterodyne transmission system that enables extremely stable and low-cost broad-band transmission in the millimeter-wave band. The system was applied to a 60-GHz-band transmission system for the first time. The transmitter of the developed system transmits RF modulated signals and a local oscillation signal simultaneously, and the receiver detects these signals by using a square-law-type detection technique, thus creating a very stable and low phase-noise millimeter-wave transmission link without the use of an expensive and more advanced frequency-stabilization technology. Since the receiver no longer requires a millimeter-wave oscillator for frequency conversion, the devices used in this system can be miniaturized and the cost of the system can be reduced. This paper discusses the performance of the developed system in terms of its phase-noise degradation and carrier-to-noise power ratio (CNR). We also discuss the optimal transmitter design to obtain the maximum CNR. Using our miniaturized monolithic millimeter-wave integrated-circuit-based 60-GHz-band experimental system, we demonstrate that our millimeter-wave transmission link is completely free of phase-noise and frequency-offset degradation due to the use of a millimeter-wave local oscillator. We show that equal transmission-power distribution between the RF signal and local carrier gives the maximum CNR under the transmission-power-limited conditions. Also, we demonstrate that QPSK-modulated satellite broadcast multichannel video signals with a 300-MHz bandwidth, in total, can be successfully transferred over a distance of 8 m.**

***Index Terms*—Carrier-to-noise power ratio, frequency-offset cancellation, millimeter wave, phase-noise cancellation, self-heterodyne, 60-GHz band, square law.**

I. Introduction

WIRELESS systems using a millimeter-wave band are expected to enable both very high-capacity wireless transmission and the miniaturization of devices used in the systems. Various kinds of millimeter-wave applications have been discussed all over the world and in Japan. They includes a high-speed wireless local area network (LAN) [1], a wireless home link (wireless IEEE 1394 transmission system) [2], a fixed wireless access system [3], and a video transmission system for households [4]–[7].

Among these, the video transmission system is the simplest millimeter-wave application because this system is a one-way redistribution system for households of received terrestrial or satellite-broadcast video signals, and we believe that it will become the first common millimeter-wave application in household use. Fig. 1 illustrates a millimeter-wave video transmission system for household use. Terrestrial, satellite-broadcast, and/or cable television (CATV) signals are redistributed throughout the house by using millimeter waves. Thus, a TV set can be placed anywhere in the house without the need for troublesome wiring.

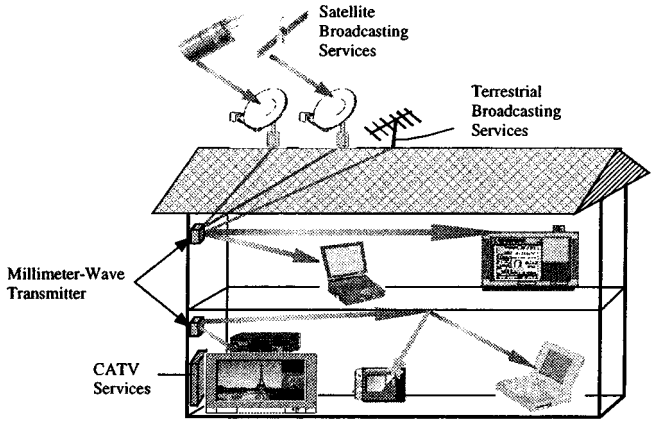

Fig. 1. Millimeter-wave video transmission system.

In spite of the existence of a very broad bandwidth [8] and a simple millimeter-wave application such as that in video transmission systems, millimeter-wave signal transmission has been very difficult to introduce and its use has not yet become common because of a serious problem that still has to be overcome. The up-conversion of a signal onto a millimeter-wave-band signal seriously deteriorates the phase-noise and frequency-stability characteristics of the transmission link and, as a result, the signal quality seriously degrades or it becomes impossible to demodulate the signal under certain conditions, especially when we transfer a signal digitally modulated by such schemes as phase-shift keying (PSK), quadrature amplitude modulation (QAM), or orthogonal frequency division multiplexing (OFDM)[10]–[12]. For example, a digital satellite broadcasting service using communication satellites (CSs), which can be a target for millimeter-wave video transmission systems, has been provided in Japan by using a bandwidth of over 500 MHz in a QPSK-modulation format. However, it requires that such systems have phase-noise characteristics of less than −52, −70, and −80 dBc/Hz for 1-, 5-, and 10-kHz frequency offset, respectively [9].

We can reduce this degradation by using a very stable millimeter-wave local oscillator with excellent phase-noise charac-

Manuscript received January 22, 2001; revised June 27, 2001.

The authors are with the Communications Research Laboratory, Independent Administrative Institution, Kanagawa 239-0847, Japan (e-mail: y-shoji@crl.go.jp).

Publisher Item Identifier S 0018-9480(02)05208-0.

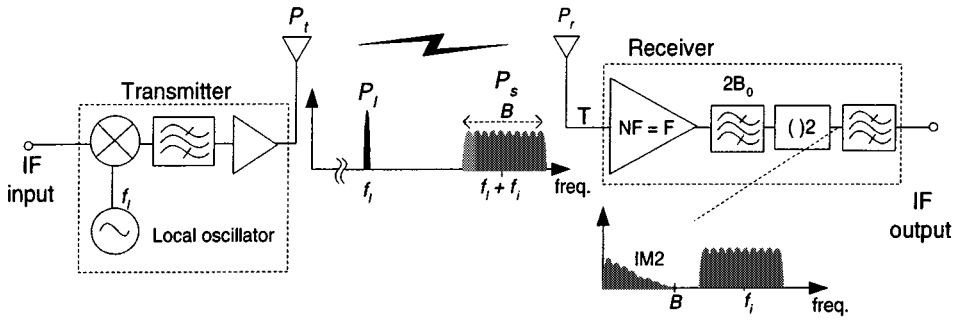

Fig. 2. Configuration of millimeter-wave self-heterodyne transmission system and receiver model.

teristics as those of an oscillator used in recent measurements. However, we found that creating such a small and stable oscillator for the millimeter-wave band is technically very difficult and expensive even with the use of an advanced frequency stabilization technique [13]–[15]. We thus concluded that it is very difficult to both miniaturize apparatus and reduce the phase-noise power well enough to enable the transmission of highly efficient digitally modulated signals if we use a conventional millimeter-wave system configuration.

A number of effective solutions to avoid the phase-noise problem have already been reported. The use of a primitive modulation technique, such as amplitude-shift keying (ASK) or frequency-shift keying (FSK), enables a millimeter-wave data-signal transmission tolerant of phase-noise and frequency offset [1], [2]. However, the use of these modulation techniques degrades the sensitivity of the receiver and efficiency of frequency. The use of differentially encoded modulation, such as differential phase-shift keying (DQPSK) combined with differential-delay detection, is effective for removing phase-noise disturbance [18]. However, this technique limits the type of modulation used and cannot be applied to millimeter-wave transmission systems that must be transparent to the modulation format, such as video transmission systems. Another effective technique is secondary modulation, whereby the carrier is modulated using amplitude or frequency modulation by modulated subcarriers, as in QAM/AM or QAM/FM systems [19], [20]. However, this technique is not suitable for low-cost broad-band signal transmission in the millimeter-wave band because currently available modulators cannot handle very broad-bandwidth signals.

To solve the above problems, we developed a millimeter-wave signal transmission system that uses a self-heterodyne detection scheme. The transmitter transmits an RF signal together with a local carrier used for up-conversion, while the receiver only down-converts the RF signal by using self-heterodyne detection, i.e., by mixing the received RF signal with the received local carrier. This system can, in principle, eliminate the effects of phase noise and frequency offset generated at the transmitter because the signal and local carrier received have the same phase-noise and frequency-offset characteristics. The self-heterodyne detection is enabled by using a square-law-type detection technique at the receiver. As will be described in Section II, this system has a very simple configuration and it can be used at a lower cost compared to that of conventional wireless systems that use a pilot-insertion technique to recover a coherent carrier at the receiver [16] or a technique of a self-oscillating mixer (SOM) [17] because it does not need a special function to insert a pilot tone at the transmitter, nor any special carrier recovery function, nor a local/reference oscillator itself at the receiver. In addition, our system does not cause any delay in recovering a phase-locked synchronized carrier, thus enabling a very fast response to the frequency jitter can be expected. However, this direct transmission of a local carrier with an RF signal is possible only if there is a very broad bandwidth where the local frequency and the RF signal are included in the signal band.

On the other hand, the millimeter-wave transmission system, especially our target unlicensed 60-GHz-band wireless system for households, is not plagued by problems of multipass fading and interference. The millimeter-wave transmission link is based on a line-of-sight path, and the use of a comparatively high-gain antenna eliminates any undesired reflected or interfering signals in most situations.

The remainder of this paper is organized as follows. Section II describes the system configuration and design requirements for a millimeter-wave self-heterodyne system, and also explains how phase noise and frequency offset are canceled. Section III analyzes the carrier-to-noise power ratio (CNR) obtained for this system, and discusses the optimal transmitter design that gives the best CNR performance under transmission-power-limited conditions. Section IV describes the results of experiments using our miniaturized millimeter-wave system, and discusses the results obtained experimentally in Section III. Section V presents the results of our experimental transmission of multichannel video broadcasting signals having a QPSK-modulation format and a 300-MHz bandwidth in total.

II. System Configuration and Principle of Operation

Fig. 2 shows the configuration of our millimeter-wave self-heterodyne transmission system. The configuration is quite similar to that of a conventional frequency up- and down-conversion system. The transmitter consists of a millimeter-wave oscillator, a mixer, a bandpass filter, and an amplifier. In our system, the transmitter simultaneously transmits a local carrier and an RF modulated signal. Therefore, the mixer, bandpass filter, and amplifier must be designed to pass both an RF modulated signal and a local carrier. In conventional frequency-conversion systems, the output of the mixer includes not only an RF signal, but also a local carrier and an image signal, and the bandpass filter following the mixer is designed to reject both. Our system, however, does not have to reject a local carrier.

As will be discussed in Section III, there is an optimal transmission-power distribution between a local carrier and an RF signal under transmission-power-limited conditions. We can easily change the power distribution by adjusting the IF input power or the frequency characteristics of the bandpass filter.

The receiver amplifies the received RF signal and local carrier and feeds them to a nonlinear device that works as a square-law detector. The RF signal is mixed there with the local carrier received, and a down-converted IF signal is obtained.

If we assume that the IF signal to be transferred is an unmodulated carrier with frequency ω_i, all the signals received at the receiver are represented by

$$r(t) = \sqrt{2P_s}\cos\left[(\omega_l+\omega_i)t+\theta_l(t)\right] + \sqrt{2P_l}\cos\left[\omega_l t+\theta_l(t)\right]+n(t) \quad (1)$$

where $P_s, P_l, \omega_l, \omega_i, \theta_l(t)$, and $n(t)$ are, respectively, the received signal power, received local-carrier power, angle frequency of the local carrier, angle frequency of the IF signal, phase-noise included in the local carrier, and receiver noise. Note that the RF signal represented by the first term in (1) includes the phase noise $\theta_l(t)$ as a result of up-conversion at the transmitter (mixing the IF signal with the local carrier). The square-law device into which these signals are fed has as its output

$$\begin{aligned} v(t) &= r^2(t) \\ &= 2P_s\cos^2\left[(\omega_l+\omega_i)t+\theta_l(t)\right] \\ &\quad + 2P_l\cos^2\left[\omega_l t+\theta_l(t)\right]+n^2(t) \\ &\quad + 2\sqrt{2P_s}n(t)\cos\left[(\omega_l+\omega_i)t+\theta_l(t)\right] \\ &\quad + 2\sqrt{2P_l}n(t)\cos\left[\omega_l t+\theta_l(t)\right] \\ &\quad + 4\sqrt{P_sP_l}\cos\left[(\omega_l+\omega_i)t+\theta_l(t)\right]\cos\left[\omega_l t+\theta_l(t)\right]. \end{aligned} \quad (2)$$

You can see from (2) that six terms appear in the output: the first term is for the signal times signal $(s\times s)$, the second one is for the local carrier times local carrier $(l\times l)$, the third one is for the noise times noise $(n\times n)$, the fourth one is for the signal times noise $(s\times n)$, the fifth one is for the local carrier times noise $(l\times n)$, and the last one is for the signal times local carrier $(s\times l)$. All these terms contain a low-frequency component with a frequency near f_i and a high-frequency component with a frequency near $2f_l$. Since all the high-frequency components can be eliminated by bandpass filtering after the square-law detection, we neglect them in the following equations.

The last term $(s\times l)$ in (2) can be reduced to the detected IF signal $v_s(t)$ as follows:

$$v_s(t) = 2\sqrt{P_sP_l}\cos\omega_i t. \quad (3)$$

You can see from (3) that the detected IF signal does not include the phase-noise term $\theta_l(t)$ and is independent of the local-carrier frequency. This means that the phase noise and frequency offset caused at the transmitter can be eliminated by using this type of detection. Furthermore, you can easily see from (3) that $P_s = P_l$ gives the highest detected IF-signal power when the total transmission power (P_s+P_l) is limited.

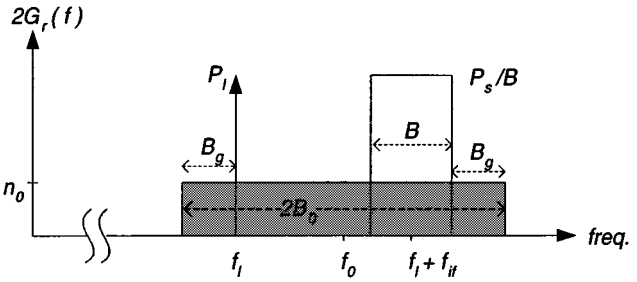

Fig. 3. One-sided power-spectrum density of a received signal.

In the above discussion, we assumed an unmodulated IF signal and proved that phase-noise- and frequency-offset-free transmission is possible. In reality, however, an IF signal has a bandwidth of $f_i-(B/2)\le f\le f_i+(B/2)$, and the $s\times s$ term in (2) generates second-order distortion components that will appear in the frequency band of $|f|\le B$, as shown in Fig. 2. Thus, it is obvious that, to keep the second-order distortion components from disturbing the detected IF signal, the IF signal for our system must satisfy the following condition: the highest frequency included must be lower than twice the lowest frequency included. This condition is represented by the following inequality:

$$f_i \ge \frac{3}{2}B. \quad (4)$$

III. Theoretical Analysis of CNR Performance

A. Derivation of Theoretical CNR Representation

To derive a theoretical representation of the CNR performance, we assume that the RF signal has a rectangular power spectrum with bandwidth B and power-spectrum-density level P_s/B (see Fig. 3).

To find the spectral contributions due to the $n\times n, s\times n$, and $l\times n$ terms, we assume that the noise is bandlimited white noise with power-spectrum-density level n_0, bandwidth $2B_0$, and center frequency f_0 (see Fig. 3). We also assume that the bandpass window passes both the RF signal and local carrier and that there is an additional guard bandwidth B_g in the upper and lower frequencies, which is the same for both frequencies, as shown in Fig. 3.

The contributions of the low-frequency components of $n\times n, l\times n$, and $s\times n$ to the two-sided power-spectrum density can be derived by considering the superposition of each power spectrum or the Fourier transform of their autocorrelation function [21]. These contributions are given by (5)–(7), shown at the bottom of the following page. Fig. 4 shows the power-spectrum density of a square-law-detected signal. Using (3) and (5)–(7), we can express the CNR of the square-law-detected IF signal as

$$\mathrm{CNR} = \frac{P_sP_l}{\int_{(f_i-(B/2))}^{(f_i+(B/2))} G_{n\times n}(f)+G_{s\times n}(f)+G_{l\times n}(f)\,df}. \quad (8)$$

Here, we assume the receiver model also shown in Fig. 2. It includes, besides the square-law detector, an antenna with equivalent noise temperature T, an amplifier with noise figure F, and a bandpass filter with bandwidth $2B_0$. If we further

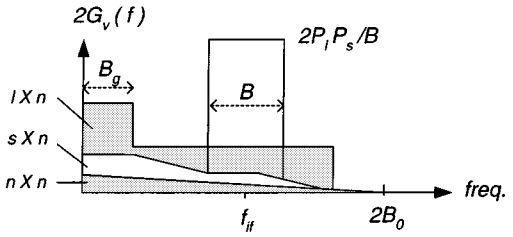

Fig. 4. One-sided power-spectrum density of a square-law-detected signal.

assume that each power spectrum of the above detected noise components $G_{n\times n}(f)$, $G_{l\times n}(f)$, and $G_{s\times n}(f)$ has bandlimited white noise shape with the peak power level shown in (5)–(7), we can reduce (8) to

$$\mathrm{CNR} = \frac{\dfrac{R_l}{(1+R_l)^2}P_r^2}{2B\left[B_0(kTF)^2 + P_r kTF\right]} \tag{9}$$

where P_r is the total received power, and R_l is the ratio of the local-carrier power to the signal power. Here, P_r and R_l are given by

$$P_r = P_t G_{\mathrm{ant}} \left(\frac{\lambda}{4\pi d}\right)^2 \tag{10}$$

and

$$R_l = \frac{P_l}{P_s}, \tag{11}$$

where $P_t, G_{\mathrm{ant}}, \lambda$, and d are, respectively, the total transmission power (i.e., the sum of the signal power and the local-carrier power), total antenna gain, wavelength, and transmission distance.

B. CNR Performance and Optimal Transmitter Design

Fig. 5 shows CNR as a function of power ratio R_l for different transmission distances. The parameters used in the calculations are listed in Table I. Note that the total transmission power was always fixed at 0 dBm. You can see from the figure that $R_l = 0$ dB gives the best CNR performance. At a point near $R_l = 0$ dB, the CNR gradually decreases as R_l leaves the 0-dB point, and an increase (or a decrease) in R_l by 10 dB degrades the CNR by 5 dB. However, an additional increase (or a decrease) in R_l by over 10 dB (i.e., at a point of $R_l = -20$ or 20 dB) causes greater CNR degradation of approximately 9 dB. As a result, we must design a transmitter that would enable equal transmission power distribution between the signal and local carrier.

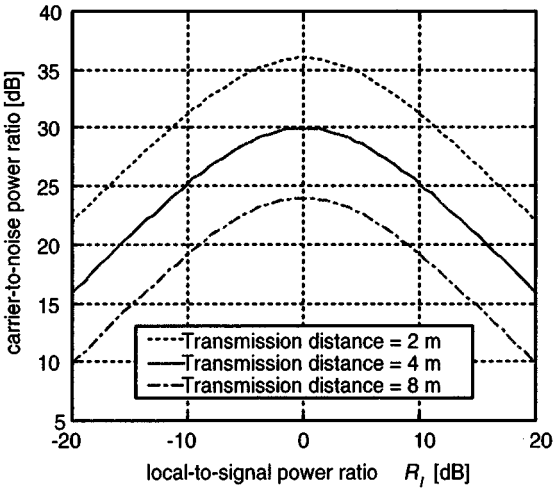

Fig. 5. CNR versus local-to-signal power ratio for different transmission distances.

TABLE I
CALCULATION PARAMETERS

Signal bandwidth B	**300 MHz**
Noise bandwidth $2B_0$	**2.5 GHz**
Noise figure of amplifier	**5 dB**
Noise temperature of receiver antenna	**300 K**
Total antenna gain	**35 dBi**

As for the CNR dependence on the transmission distance, you can see from Fig. 5 that doubling the transmission distance decreases the CNR by 6 dB. This rule is the same as that for a conventional down-conversion-type receiver equipped with a local oscillator, and may be easily acceptable because doubling the transmission distance causes an additional transmission loss of 6 dB. Note, however, that our result comes from the fact that doubling the transmission distance causes a 12-dB decrease in the detected signal power, but also a 6-dB decrease in the detected noise level as well, as seen in (9). In addition, note that this rule can be applied only if the noise power before the

$$G_{n\times n}(f) = \begin{cases} 2B_0 n_0^2(1 - |f|/2B_0), & f \le |2B_0| \\ 0, & \text{elsewhere} \end{cases} \tag{5}$$

$$G_{l\times n}(f) = \begin{cases} 2P_l n_0, & |f| \le B_g \\ P_l n_0, & B_g \le |f| \le 2B_0 - B_g \\ 0, & \text{elsewhere} \end{cases} \tag{6}$$

$$G_{s\times n}(f) = \begin{cases} 2P_s n_0, & |f| \le B_g \\ P_s n_0\left(2 - \frac{|f|-B_g}{B}\right), & B_g \le |f| \le B_g + B \\ P_s n_0, & B_g + B \le |f| \le 2B_0 - (B_g + B) \\ P_s n_0\left(1 - \frac{|f|-B_0+(B_g+B)}{B}\right), & 2B_0 - (B_g + B) \le |f| \le 2B_0 - B_g \\ 0, & \text{elsewhere.} \end{cases} \tag{7}$$

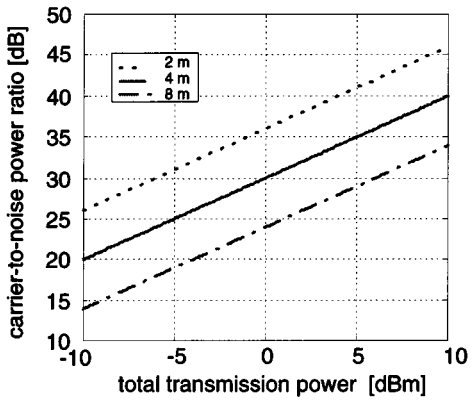

Fig. 6. CNR versus total transmission power for different transmission distances.

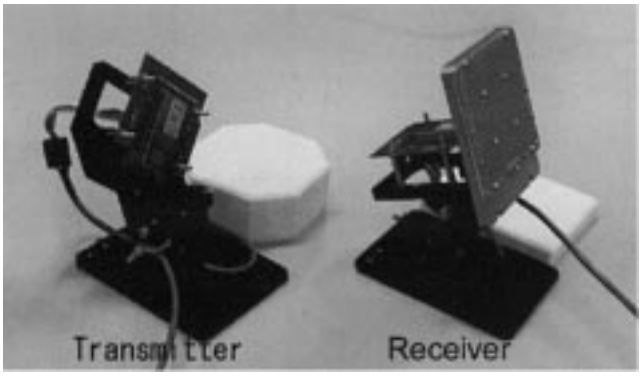

Fig. 7. Transmitter and receiver.

square-law detection dominates the CNR performance in the receiver. If the conversion loss of the square-law detection is large and the noise power after the detection dominates the CNR performance, doubling the distance, therefore, decreases the CNR by 12 dB.

Fig. 6 shows CNR as a function of the total transmission power for different transmission distances when $R_l = 1$. You can see from this figure that the CNR is proportional to the total transmission power, and a CNR of 34 dB can be obtained with a 10-dBm transmission power under the conditions shown in Table I.

Finally, we will consider the case when $P_r \gg B_o kTF$ and $R_l = 1$. Here, (9) can be simplified as follows:

$$\mathrm{CNR} \simeq \frac{P_r}{8BkTF} = \frac{P_t G_{\mathrm{ant}} \left(\dfrac{\lambda}{4\pi d}\right)^2}{8BkTF}. \tag{12}$$

This means that the CNR obtained with this self-heterodyne detection system using a square-law-type detection technique is essentially 9 dB worse than that obtained with a conventional down-conversion-type receiver having the same noise figure, and that the CNR is reduced by 6 dB if the range is doubled, which is what can be expected in conventional up- and down-conversion systems.

IV. Experimental Demonstration Using 60-GHz-Band GaAs MMIC-Based System

A. Experimental Setup

Fig. 7 depicts a photograph of the RF transmitter and receiver, and Fig. 8 shows our experimental setup. The RF transmitter used was a GaAs monolithic millimeter-wave-integrated circuit (MMIC)-based RF module that included a voltage-controlled oscillator (VCO), frequency doubler, mixer, bandpass filter, and amplifiers in one $50 \times 23 \times 6.5$ mm package [5], [22]. This RF module was originally developed as a general millimeter-wave up-converter module. Thus, local and image components are rejected at the output. For our purposes, we tuned a transmitter to transmit both a local carrier and a signal by choosing a bandpass filter with gradual cutoff characteristics to pass the local frequency. The VCO was a dielectric-resonator oscillator (DRO) and its phase-noise characteristics after doubling the frequency are shown in Fig. 9. A patch antenna with a gain of 5 dBi and wide-beam characteristics was also included in the transmitter module. The two-sided 3-dB angle of the antenna was approximately 90°.

The receiver was a similar GaAs MMIC-based RF module, which was also developed as a general millimeter-wave down-converter that can accept an external local oscillator. However, in our experiment, we used the receiver without inserting any local-oscillator signal. As a result, the FET-type mixer in the receiver module worked as a square-law device. RF signals were received with a dielectric-resonator antenna with a gain of 30 dBi, and fed to this RF module. The beamwidth of the receiver antenna was very narrow and its two-sided 3-dB angle was less than 5°. This configuration enabled the receiver to avoid receiving signals from an undesired reflected path and accept only the desired line-of-sight path signals generated at the transmitter.

We used two measurement-signal generators (HP8648C) to generate transmitted signals in the IF band. We used a spectrum analyzer (HP8565E) with a phase-noise measurement utility (HP85671A) and an external IF-band amplifier to measure the carrier power and phase-noise characteristics at the receiver side.

In the first step of our experiments, we carefully pointed the receiver antenna at the transmitter by transferring an unmodulated carrier and adjusting the antenna direction to obtain the maximum IF detected power. This pointing was not so difficult to do despite the use of such a high-gain antenna because the transmitter-antenna pattern was very broad and we had to carefully adjust only the receiver side. Some important specifications of the experimental setup are listed in Table II.

B. Demonstration of Phase-Noise Cancellation

First, we observed phase-noise cancellation. We input a single IF carrier with a 1.5-GHz frequency to the transmitter, and measured its phase-noise characteristics and those of the IF output carrier detected at the receiver when the transmission distance was 4 m. The phase-noise characteristics of the IF input and IF output carriers are shown in Figs. 10 and 11, respectively. Table III lists their phase-noise power at several frequency-offset points.

By comparing Figs. 11 and 10 or the values listed in Table III, you can find that the phase-noise characteristics of the IF output carrier deteriorated much less compared with those of the IF

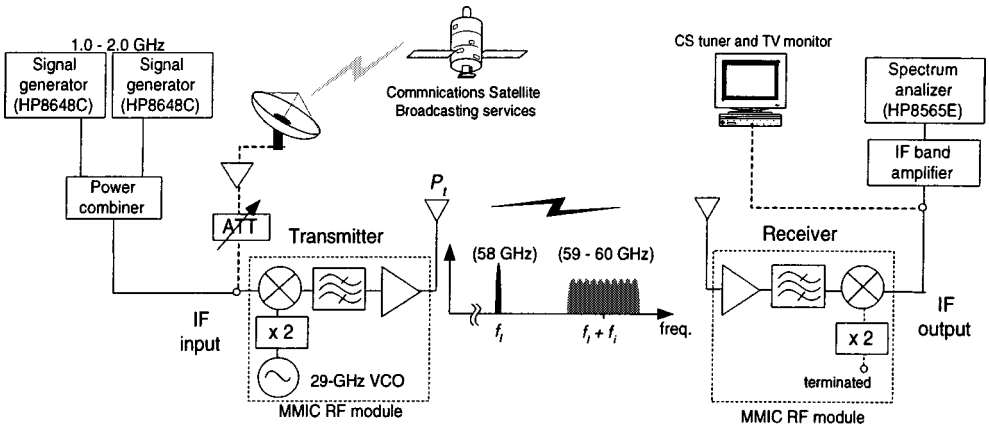

Fig. 8. Experimental setup.

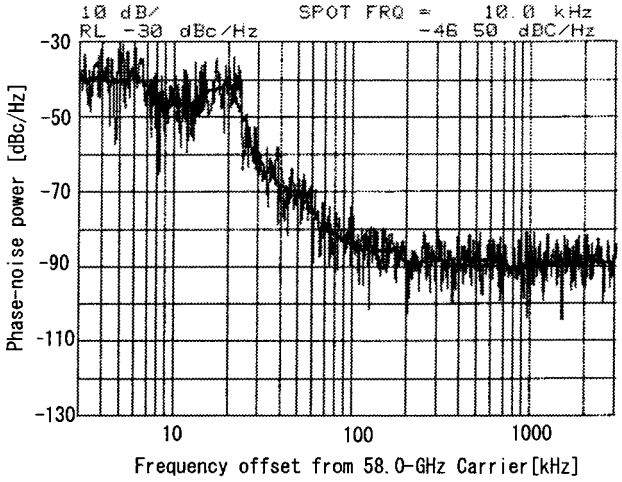

Fig. 9. Phase-noise characteristics of millimeter-wave local carrier.

TABLE II
EXPERIMENTAL SETUP

Local frequency	58 GHz
RF frequency	59 – 60 GHz
IF frequency	1 – 2 GHz
Total gain of the transmitter	20 dB @1.5GHz input
Receiver noise figure	8 dB
Transmitter antenna gain	5 dBi
Receiver antenna gain	30 dBi
Transmission distance	4 or 8 m

input carrier in spite of much more inferior phase-noise characteristics of the millimeter-wave local carrier. These results demonstrate that the additional phase noise caused at the transmitter was successfully canceled by self-heterodyne detection, as explained in Section II. You can also see from Table III that the phase-noise power at a 10-kHz frequency offset was less than −100 dBc/Hz after millimeter-wave transmission. To the best of our knowledge, this value represents the best performance for all 60-GHz-band transmission systems [13]–[15]. Furthermore, we know that this value was restricted by the phase-noise characteristics of the IF signal generator we used, and we believe that we can attain much better phase-noise characteristics with this transmission system.

TABLE III
COMPARISON OF PHASE-NOISE CHARACTERISTICS (UNIT: dBc/Hz)

Offset freq. (kHz)	0.1	1	5	10
IF input carrier	-87	-92	-99	-104
IF output carrier	-84	-93	-97	-103

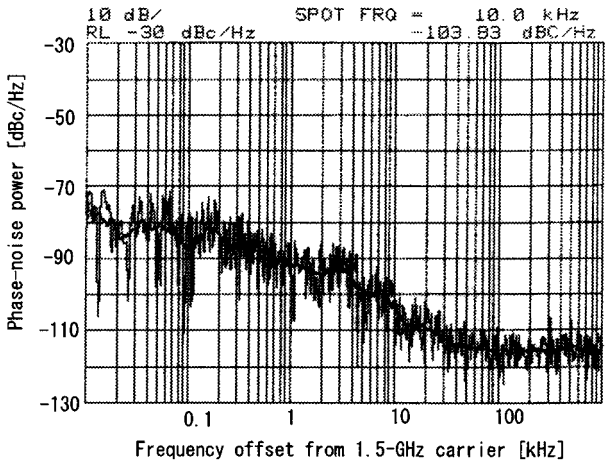

Fig. 10. Phase-noise characteristics of IF input carrier.

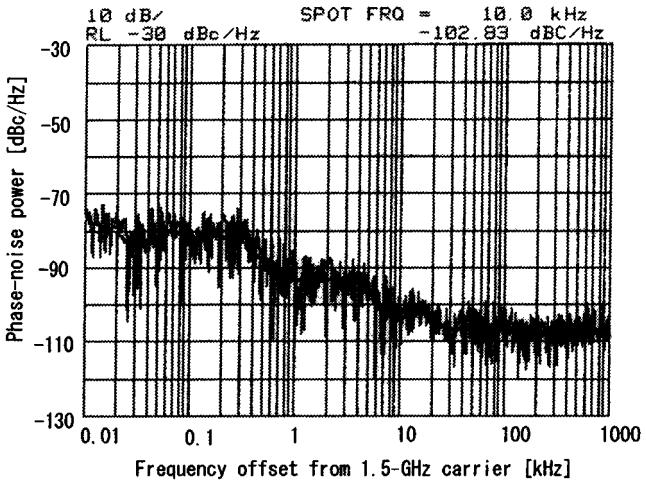

Fig. 11. Phase-noise characteristics of detected IF output carrier.

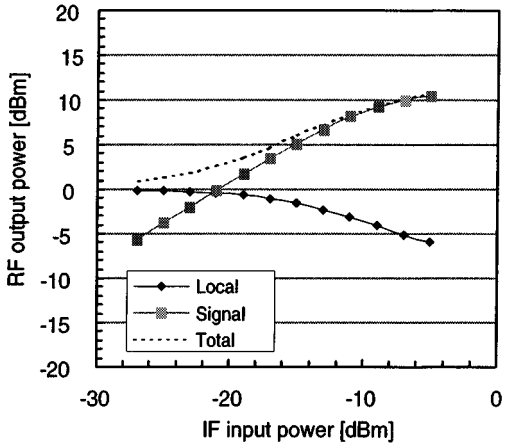

Fig. 12. I/O characteristics of millimeter-wave transmitter.

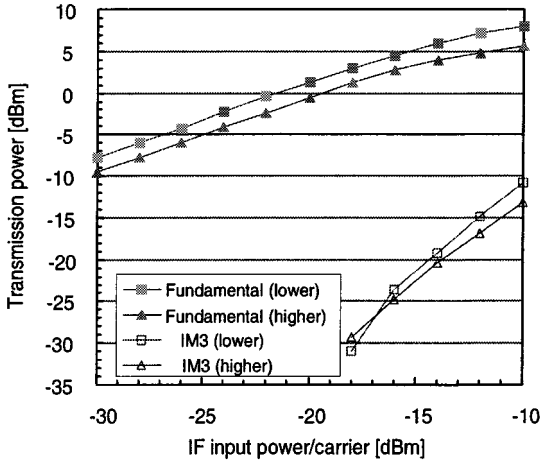

Fig. 13. IM3 performance of millimeter-wave transmitter.

C. Measurements of Link Performance

Before we investigated the link performance of our experimental system, we measured the I/O characteristics of the transmitter. The transmission power for the signal carrier and that for the local carrier are plotted in Fig. 12 against the IF input power. An IF frequency of 1120 MHz was used, and the RF transmission powers were calculated from the received powers measured using a standard gain horn antenna and a spectrum analyzer with a preselected RF section (HP11974V). You can see from this figure that the signal power increased linearly as the IF input power increased, while the local power decreased because of the saturation effects of the mixer and amplifier in the transmitter. The total transmission power is also plotted in this figure, and you can see that it gradually increased with an increase in the IF input power.

Fig. 13 presents the I/O characteristics of the transmitter. We investigated the third-order intermodulation distortion (IM3) performance of the transmitter by conducting a two-tone test. The IF frequencies used for the two-tone test were 1100 and 1140 MHz. Although the output power of the higher fundamental carrier was lower by about 2 dB than that of the lower fundamental carrier because of the frequency characteristics of the millimeter-wave amplifier in the transmitter, you can see from this figure that the suppression level (the signal level minus the IM3 level) was higher than 30 dB when the input power per carrier was −18 dBm. From this result, we can estimate the minimum carrier-to-interference power ratio (CIR) for the transmitter when it transmits multichannel signals [6], [23]. For example, we estimated that eight carriers can be transmitted with a minimum CIR of over 30 dB when we choose an IF input power of −26 dBm/carrier.

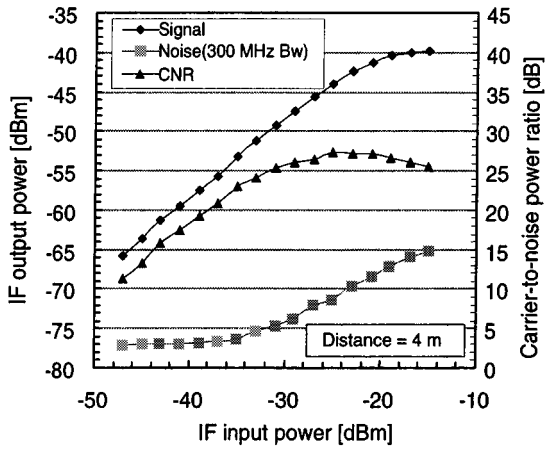

Fig. 14. Detected IF output power and CNR performance (4 m).

The CNR and IF output power measured when the distance was 4 m are plotted against the IF input power in Fig. 14. The noise power in the 300-MHz bandwidth is also shown in this figure. The IF frequency was 1120 MHz. You can see from this figure that both the signal and noise power increased linearly when the IF input power was over −30 dBm. (Remember that if you use a general down-converter, the detected noise power is independent of the received power.) This result is consistent with the result of the theoretical analysis discussed in Section III.

You can also see from Fig. 14 that the CNR was saturated when the IF input power was around −30 dBm, and it reached a peak when the IF input power was −25 dBm. With the larger IF input power, the CNR gradually decreased. As discussed in Section III, the CNR was determined by the total transmission power and the power distribution between the local carrier and RF signal. When the IF input power was over −20 dBm, the transmission power gradually increased, but the power difference between the local carrier and RF signal also increased, as shown in Fig. 12. This concluded that the CNR did not improve even though the total transmission power increased.

According to our theoretical results shown in Fig. 6, a CNR of 33 dB was obtained when the total transmission power was 3 dBm and the distance was 4 m. In our experiments, a CNR of 27 dB was obtained in our experimental system under the same conditions (when the IF input power was −21 dBm). Thus, there was a CNR difference of 6 dB. This difference is not so big if we consider that the noise figure in the experimental system was worse by 3 dB than that in the theoretical model.

Fig. 15 plots the CNR and IF output power against the IF input power when the distance was 8 m. The noise power in the 300-MHz bandwidth is also shown in this figure. The curves obtained for each of these characteristics are not so different from those in Fig. 14, but it is interesting to compare the CNR obtained for the 4-m distance to that obtained for the 8-m distance. When the same IF input power of −21 dBm was input

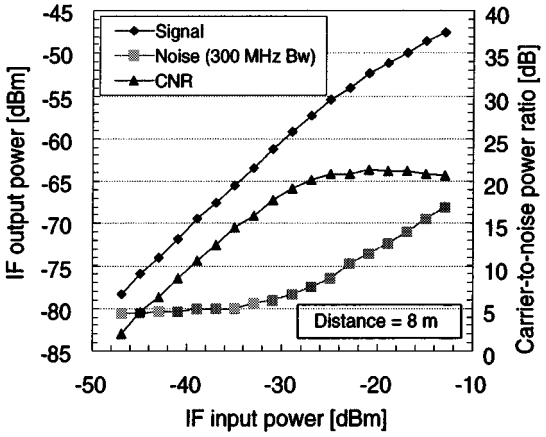

Fig. 15. Detected IF output power and CNR performance (8 m).

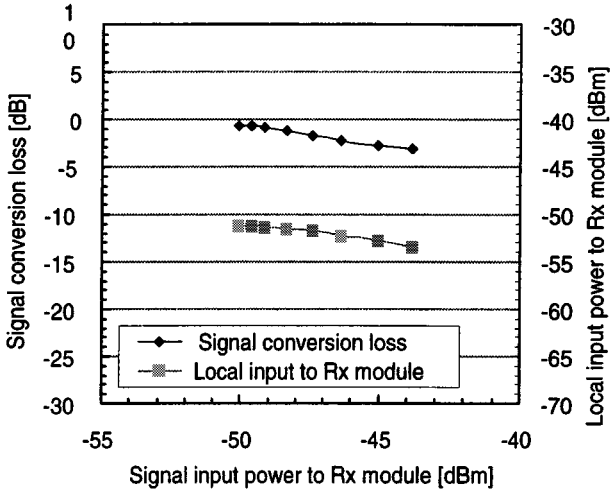

Fig. 16. Conversion-loss characteristics of the receiver.

to the transmitter, the CNR's obtained for the 4- and 8-m distances were 27 and 21 dB, respectively. These results are consistent with our theoretical results that doubling the distance effectively reduces the CNR by 6 dB.

Although we used an MMIC-based RF receiver developed as a general down-converter, improving the conversion efficiency and optimizing the design of the RF receiver are important. Fig. 16 shows the conversion loss of our receiver against the signal power input to the receiver. It also shows the corresponding local carrier power input to the receiver. The signal and local carrier powers input to the receiver were calculated from the transmission powers shown in Fig. 12 and (10). The conversion loss was then obtained by comparing the detected IF output power in Fig. 15 and the RF signal power input to the receiver. You can see that the conversion loss was greater than -4 dB and it appears to be almost proportional to the local power input to the receiver. We think that the conversion loss of the receiver used in our experiments is not sufficient for our purposes if we consider that an amplifier with approximately 30-dB gain is included in the receiver module. An increase in the conversion loss can deteriorate the received CNR performance even further because the noise figure after square-low detection dominates the CNR in this case. Therefore, in the near

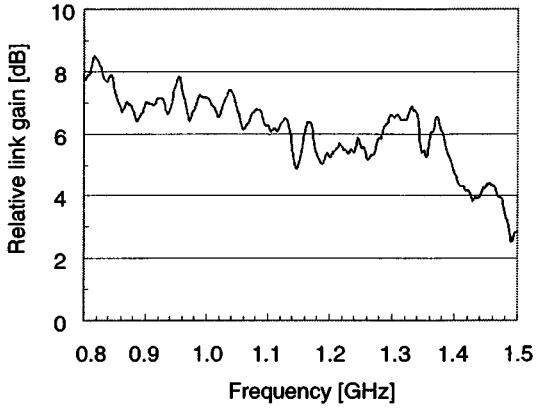

Fig. 17. $S21$ frequency characteristics.

TABLE IV
CS SERVICE SIGNALS

RF frequency band	12.2 - 12.75 GHz
modulation	QPSK
bandwidth/channel	27 MHz
bit rate	42.192 Mbps
coding for video signals	MPEG-2Video
outer code	RS(204,188)
inner code	convolution code (1/2 - 7/8)
1st local frequency	11.2 GHz
required CNR	more than 8 dB

future, we will focus on improving the conversion efficiency of our receiver.

Fig. 17 shows the $S21$ frequency characteristics of the experimental transmission link measured by a network analyzer (HP8753E) when the transmission distance was 4 m. As you can see, the transmission link had broad-band transmission characteristics ranging from 800 MHz to 1.5 GHz, and the operation of the self-heterodyne system using a square-law detection technique was successful with the maximum link-gain deviation of less than 6 dB.

D. Transmission Experiment of Multichannel Digital Broadcasting Signals

We present at the end of this section the results of a transmission experiment for multichannel digital broadcasting signals. The experimental setup is shown in Fig. 8. In Japan, there are two types of satellite broadcasting services. One is a broadcasting-satellite (BS) service, which uses analogous frequency modulation, and the other is a communications-satellite (CS) service, which uses digital QPSK modulation. Last year, we were able to transfer BS signals with a millimeter-wave band by using a miniaturized experimental system that was very similar to our experimental system described in this paper, except that it was not a self-heterodyne system. However, at that time we were not able to transfer CS signals because of the phase noise of the millimeter-wave local oscillator, unless we use a measurement equipment signal generator as a local oscillator [24]. We will now discuss the transmission of CS signals using a miniaturized system where a DRO was used as a local oscillator. Some specifications for the CS signals we used are listed in Table IV.

Fig. 18. Picture with a CNR of 7 dB.

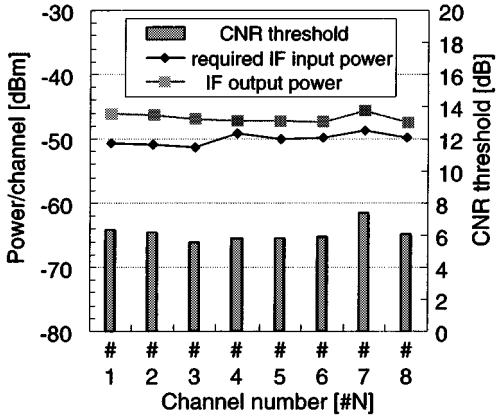

Fig. 19. Minimum required IF input power and the CNR threshold.

In the experiment, we prepared nine channels of broadcasting signals in the IF band by receiving the signals with a parabolic-antenna set that included a down-converter. Their powers were then amplified, properly attenuated, and input to our RF transmitter as shown in Fig. 8. The IF video signals detected at the RF receiver were directly input to the CS tuner (CS Digital Tuner CDT600D, Maspro Corporation, Aichi, Japan). We investigated the quality of the video signals by watching images on a TV monitor.

First, we found that the quality of the picture on the TV monitor suddenly began to deteriorate when the CNR became less than 8 dB because of the use of forward error correction (FEC). When the CNR was around 7 dB, we could sometimes find a block error in the picture, as shown in Fig. 18. Finally, at the CNR of about 6 dB, a warning in Japanese, i.e., "We cannot receive signals," appeared on the monitor. Thus, we made this last state the threshold of quality in our experiment.

We investigated the minimum IF input power and the received CNR at which the quality of the picture deteriorated beyond the above threshold for eight channels chosen from the nine channels. Fig. 19 shows the minimum IF input power, IF output power, and CNR threshold with this IF input power for each channel. You can see from this figure that the CNR threshold for most channels was approximately 6 dB and the quality of the video signals was deteriorated predominantly by the CNR. Only for channel 7 was the CNR threshold greater than 7 dB.

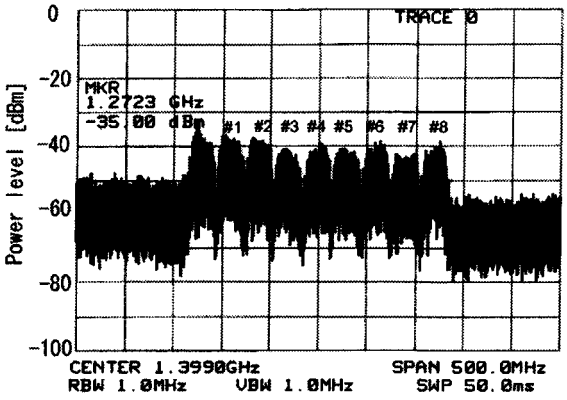

Fig. 20. Spectrum of CS signals after millimeter-wave transmission.

We think that the deviation in the frequency gain characteristics of the band resulted in this increase of the required CNR by 1 or 2 dB. However, the investigation of this phenomenon is beyond the scope of our study.

The spectrum of the detected signals for a transmission distance of 8 m is shown in Fig. 20, where the IF input power of the video signals input to the RF transmitter was approximately −15 dBm in total. In this state, the quality of all video channels was very good, and a CNR of over 20 dB was obtained for all the channels.

V. Conclusion

The millimeter-wave remote self-heterodyne system described in this paper can provide a super-stable and low-cost millimeter-wave transmission link, where the transmitter transmits a local carrier and an RF signal, and the receiver simply detects the signal by using a square-law detection technique. The configuration of the system is very simple and the system can easily be miniaturized. The transmitter can use an economical millimeter-wave local oscillator; the receiver does not need a millimeter-wave oscillator; and the configuration of the system is very similar to that of conventional millimeter-wave up- and down-conversion systems with no special function for frequency stability.

We have theoretically proven the principle of phase-noise and frequency-offset cancellation, analyzed the CNR performance obtained for this system, and discussed the optimal transmitter design that gives the best CNR. The following theoretical results were obtained.

- The system can completely eliminate the phase noise and frequency offset caused by frequency conversion at the millimeter-wave transmitter.
- The noise power detected at the receiver depends on the received signal power and proportionally increases when the received power increases.
- The CNR performance depends not only on the received total power, but also on the transmission-power distribution between the local carrier and RF signal.
- Equal transmission-power distribution between the local carrier and RF signal gives the best CNR performance under transmission-power-limited conditions.
- Doubling the transmission distance results in a 12-dB degradation of the detected power for the signal, along

with a 6-dB degradation for the noise level. Thus, doubling the distance degrades the CNR by 6 dB.
- Our system suffers from an unavoidable CNR degradation of 9 dB when compared to conventional up- and down-conversion-type transmission systems.
- A 300-MHz-bandwidth signal can be transferred over an 8-m distance with a CNR of 34 dB if the transmitter design is optimized.

In the experiment using our developed miniaturized MMIC-based system, the phase noise was effectively canceled, which allowed us to easily achieved phase-noise degradation-free transmission in the 60-GHz band. As a result of our link performance measurements, we found that doubling the distance causes CNR degradation of 6 dB and that the CNR is dependent not only on the received total power, but also on the power distribution between the local carrier and RF signal. When we transferred an unmodulated carrier over a distance of 8 m with 3-dBm transmission power, we obtained a CNR of over 20 dB for a 300-MHz noise bandwidth. This value of CNR was not far from our theoretical estimation. To show the feasibility of our system, we successfully transmitted QPSK-modulated multichannel digital video signals with a 300-MHz bandwidth over an 8-m distance.

ACKNOWLEDGMENT

The authors thank the Millimeter-Wave Video-Transmission-Systems Collaboration Group, Yokosuka Research Park (YRP), Yokosuka, Japan, for providing the equipment used in this study.

REFERENCES

[1] G. Wu, Y. Hase, and M. Inoue, "An ATM-based indoor millimeter-wave wireless LAN for multimedia transmissions," *IEICE Trans. Commun.*, vol. E83-B, no. 8, Aug. 2000.

[2] K. Ohata, K. Maruhashi, J. Matsuda, M. Ito, W. Domon, and S. Yamazaki, "A 500 Mbps 60 GHz-band transceiver for IEEE 1394 wireless home networks," in *Proc. 30th European Microwave Conf.*, Paris, France, Oct. 2000, pp. 289–292.

[3] T. Tanuma, "Current frequency management and utilization of millimeter-wave band in Japan," in *Proc. Topical Millimeter Waves Symp.*, Yokosuka, Japan, Mar. 2000, pp. 11–14.

[4] K. Hamaguchi, Y. Shoji, H. Ogawa, H. Sato, K. Tokuda, Y. Hirachi, T. Iwasaki, A. Akeyama, K. Ueki, and T. Kizawa, "A wireless video home-link using 60 GHz band: Concept and performance of the developed system," in *Proc. 30th European Microwave Conf.*, Paris, France, Oct. 2000, pp. 293–296.

[5] Y. Amano, E. Suematsu, Y. Hirachi, H. Nakano, K. Ueki, H. Ogawa, and T. Matsui, "A wireless video home-link using 60 GHz band—Transmitter/receiver," in *Proc. 30th European Microwave Conf.*, Paris, France, Oct. 2000, pp. 297–300.

[6] E. Kawakami, K. Tokuda, Y. Shoji, K. Hamaguchi, and H. Ogawa, "A wireless video home-link using 60 GHz band: A study of nonlinear distortion," in *Proc. 30th European Microwave Conf.*, Paris, France, Oct. 2000, pp. 301–304.

[7] S. Nishi, K. Hamaguchi, T. Matsui, and H. Ogawa, "A wireless video home-link using 60 GHz band: A proposal of antenna structure," in *Proc. 30th European Microwave Conf.*, Paris, France, Oct. 2000, pp. 305–308.

[8] "Technical requirements for radio equipment using 60 GHz band," Ministry of Posts Commun., Telecommun. Technol. Council, Yokosuka, Japan, Tech. Rep., Feb. 2000.

[9] *Digital Receiver for Digital Satellite Broadcasting Services Using Communication Satellites*, ARIB STD-B1, May 1996.

[10] L. Tomba and W. A. Krzymien, "Sensitivity of the MC-CDMA access scheme to carrier phase noise and frequency offset," *IEEE Trans. Veh. Technol.*, vol. 48, pp. 1657–1665, Sept. 1999.

[11] L. Tomba, "On the effect of wiener phase noise in OFDM systems," *IEEE Trans. Commun.*, vol. 46, pp. 580–583, May 1998.

[12] T. Pollet, M. V. Bladel, and M. Moeneclaey, "BER sensitivity of OFDM systems to carrier frequency offset and wiener phase noise," *IEEE Trans. Commun.*, vol. 43, pp. 191–193, Feb. 1995.

[13] K. Sakamoto, T. Kato, S. Yamashita, and Y. Ishikawa, "A millimeter wave DR–VCO on planar type dielectric resonator with small size and low phase noise," *IEICE Trans. Electron.*, vol. E82-C, no. 1, pp. 119–125, Jan. 1999.

[14] H. Wang, K. W. Chang, L. T. Tran, J. C. Cowles, T. R. Block, E. W. Lin, G. S. Dow, A. K. Oki, D. C. Streit, and B. R. Allen, "Low phase noise millimeter-wave frequency sources using InP-based HBT MMIC technology," *IEEE J. Solid-State Circuits*, vol. 31, pp. 1419–1425, Oct. 1996.

[15] T. Kaneko, K. Tanji, Y. Amamiya, T. Niwa, H. Shimawaki, S. Tanaka, and K. Wasa, "Design and fabrication of a millimeter-wave MMIC HBT VCO with consideration for modulation linearity and low phase noise," *NEC Res. Dev.*, vol. 41, no. 1, pp. 44–48, Jan. 2000.

[16] M. Galanbari and K. Feher, "Design and experimental test and evaluation of a pilot tone aided carrier recovery system for wireless personal communications," *IEEE Trans. Consumer Electron.*, vol. 41, pp. 809–814, Aug. 1995.

[17] M. Sironen, Y. Qian, and T. Itoh, "A subharmonic self-oscillating mixer with integrated antenna for 60-GHz wireless applications," *IEEE Trans. Microwave Theory Tech.*, vol. 49, pp. 442–450, Mar. 2001.

[18] I. Bar-David, "Direct differential detection of phase-shift-keyed signals: A local-oscillator-less DPSK receiver," in *Proc. IEE Optelectron.*, vol. 141, Feb. 1994, pp. 38–42.

[19] K. Maeda and S. Komaki, "Error statistics of 64-QAM signal in AM/64-QAM hybrid optical transmission," *J. Lightwave Technol.*, vol. 18, pp. 1348–1354, Oct. 2000.

[20] S. Matsui, K. Suto, and K. Kikushima, "A novel optical receiver for AM/QAM/FM hybrid SCM video distribution systems," *IEICE Trans. Commun.*, vol. 76, no. 9, pp. 1159–1168, Sept. 1993.

[21] M. Schwartz, W. R. Bennett, and S. Stein, *Communication Systems and Techniques*. Piscataway, NJ: IEEE Press, 1996.

[22] Y. Hirachi and S. Kuroda, "Status of millimeter-wave MMIC's and their applications in Japan," in *Proc. Gallium Arsenide & Other Semiconduct. Applicat. Symp.*, Oct. 2000, pp. 369–372.

[23] J. R. Wescott, "Investigation of multiple F.M./F.D.M. carriers through a satellite T.W.T. operating near to saturation," *Proc. Inst. Elect. Eng.*, vol. 14, pp. 726–740, June 1967.

[24] Y. Shoji, Y. Amano, E. Kawakami, Y. Hirachi, E. Suematsu, K. Hamaguchi, and H. Ogawa, "Development of millimeter-wave video transmission system (6) results of BS · CS transmission experiment," in *Proc. Topical Millimeter Waves Symp.*, Yokosuka, Japan, Mar. 2000, pp. 209–212.

Yozo Shoji (S'98–M'99) received the B.E. and M.E. degrees in electrical engineering and the D.E. degree in communications engineering from Osaka University, Osaka, Japan, in 1995, 1996, and 1999, respectively.

He is currently a Researcher with the Communications Research Laboratory, Independent Administrative Institution, Kanagawa, Japan, where he has been engaged in research on millimeter-wave multimedia communication systems and microwave photonics communication systems.

Kiyoshi Hamaguchi (M'00) studied electrical engineering at the Science University of Tokyo, Tokyo, Japan, and Osaka University, Osaka, Japan. He received the Dr.Eng. degree in land mobile radio communications from Osaka University, Osaka, Japan, in 2000.

From 1991 to 1993, he was with the Radio Products Division, Anritsu Corporation, Kanagawa, Japan. Since 1993, he has been with the Communications Research Laboratory, Independent Administrative Institution, Kanagawa, Japan, where he has been engaged in the research of digital land mobile radio communications and wireless multimedia communication systems.

Hiroyo Ogawa (M'84) received the B.S., M.S., and Dr.Eng. degrees in electrical engineering from Hokkaido University, Sapporo, Japan, in 1974, 1976, and 1983, respectively.

In 1976, he joined the Yokosuka Electrical Communication Laboratories, Nippon Telegraph and Telephone Public Corporation, Yokosuka, Japan. He was engaged in the research and development on microwave and millimeter-wave integrated circuits, monolithic integrated circuits, and subscriber radio systems. From 1985 to 1986, he was a Post-Doctoral Research Associate at the University of Texas at Austin (on leave from NTT). From 1987 to 1988, he was involved with the design of the subscriber radio equipment at the Network System Development Center, NTT. From 1990 to 1992, he was involved in the research of optical/microwave monolithic integrated circuits and fiber-optic links for millimeter-wave personal communication systems at ATR Optical and Radio Communication Research Laboratories. From 1993 to 1998, he was involved with microwave photonics and microwave and millimeter-wave signal-processing techniques for CS at NTT Wireless Systems Laboratories. In July 1998, he joined the Communication Research Laboratory, Ministry of Posts and Telecommunications, Yokosuka, Japan, where he has been involved with the research and development of wireless multimedia access systems. He was an Associate Editor of the *IEICE Transactions on Electronics* (1990–1992).

Dr. Ogawa is a member of the Institute of Electronics, Information and Communication Engineers (IEICE), Japan. He serves on the IEEE Microwave Theory and Techniques Society (IEEE MTT-S) Symposium Technical Committee and is a member of the IEEE MTT-S Technical Committee and Microwave Photonics (MWP) Steering Committee. He was the secretary/treasurer of the IEEE MTT–Tokyo Chapter (1991–1992), secretary of the IEICE Microwave Technical Group as a in 1993–1994, IEICE Microwave Photonics Technical Group (1995–1998), and the secretary of the International Topical Meeting on Microwave Photonics (1996). He was also the chair of the Technical Program Committee of the 1998 Asia–Pacific Microwave Conference.